



## An *in-situ* synchrotron study on microplastic flow of electrodeposited nanocrystalline nickel



Pradipta Ghosh<sup>a,b,\*</sup>, Steven Van Petegem<sup>c</sup>, Helena Van Swygenhoven<sup>c,d</sup>, Atul H. Chokshi<sup>a</sup>

<sup>a</sup> Indian Institute of Science, Bangalore 560012, India

<sup>b</sup> Erich Schmid Institute of Materials Science, Leoben 8700, Austria

<sup>c</sup> Swiss Light Source, Paul Scherrer Institute, Villigen, Switzerland

<sup>d</sup> Neutrons and X-rays for Mechanics of Materials, IMX, Ecole Polytechnique Federale de Lausanne, CH-1012 Lausanne, Switzerland

### ARTICLE INFO

#### Keywords:

Nanocrystalline  
Recovery  
Deformation  
Root-mean-square strain  
Texture

### ABSTRACT

Deformation in nanocrystalline (NC) materials is strongly influenced by the presence of a large fraction of grain boundaries. We present a comparative study on the role of intragranular root-mean-square strain and crystallographic texture on recovery processes. The detailed microstructure analysis with conventional X ray diffraction and *in-situ* synchrotron measurements during deformation are used to understand the various attributes of recovery mechanisms associated with annealing and deformation of electrodeposited NC nickel (grain size = 30 nm). Our results emphasize the dominance of local atomic rearrangements during thermal recovery processes, while deformation induced recovery processes are supported primarily by large-scale dislocation activity. The *in-situ* deformation of NC samples with two different textures illustrates further the influence of grain boundary character on recovery processes.

### 1. Introduction

Nanocrystalline (NC) metals exhibit a high volume fraction of grain boundaries (GBs) that have an important influence on their physical properties. Their deformation behavior has been attributed variously to diffusion [1–4], dislocation emission or absorption at GBs [5], grain boundary sliding (GBS) [6,7], grain rotation [8,9], twinning and stacking faults [10–12] and grain boundary migration [13–15]. Molecular dynamics (MD) simulations [3,16–19] have suggested that the relevance of any particular deformation process depends on the grain size, the structural state of the GBs and impurity content.

The development of new advanced *in situ* synchrotron x-ray and neutron diffraction techniques in the last two decades has resulted in various important breakthrough results [20–26]. In particular, the study of intergranular lattice strain evolution during straining provides useful insights into possible deformation mechanisms. For instance, uniaxial tensile deformation along a loading direction leads to a reduction in lattice spacing along the transverse direction, related to the Poisson effect. However, as a consequence of elastic and plastic anisotropy this reduction depends on the crystallographic orientation of the grain families. For most non-textured elastically anisotropic face-centered cubic (fcc) metals undergoing intragranular dislocation slip in uniaxial tension, a tensile shift for the (200) diffraction family and a compressive shift for the (220) family in transverse direction has been

observed [26]. This is usually explained by the necessary strain compatibility between soft and hard grain families.

For NC fcc metals, however, the observed trend in lattice strain evolution during loading is not so clear [21–25]. In NC Ni–Fe (average grain size  $d = 9$  nm) [21] it was found that all grain families undergo a tensile shift upon yielding. For NC Ni with a mean grain size of 29 nm [23], a compressive shift was observed for nearly all diffraction groups. However, Cheng et al. [22] reported no notable shift up to 2% plastic strain for NC Ni with a grain size of 20 nm. An MD-informed quantized crystal plasticity simulation scheme was developed to understand the possible source for these differences [27,28]. Such simulations showed that in addition to grain size, the nature and distribution of pre-existing internal strains can significantly influence the mechanical and diffraction footprints of NC materials.

The different microstructural characteristics such as texture, GB character, grain size distribution and root-mean-square (RMS) strain of NC materials are an outcome of the used processing routes, and it is difficult to control or monitor their individual effects on deformation processes. However, it is generally noted that NC metals have significantly higher RMS strains compared to coarse-grained materials [29,30]. Transmission electron microscopic studies [31] and *in-situ* synchrotron studies [32] have shown that annealing of NC Ni up to 423 K causes a relaxation of the microstructure and thus a reduction in RMS strain, without any significant grain growth. MD simulations

\* Corresponding author at: Erich Schmid Institute of Materials Science, Leoben, Austria.

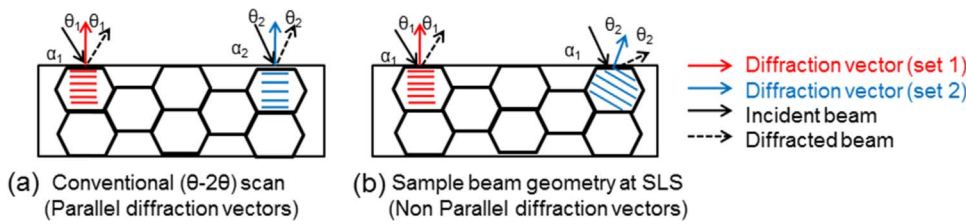


Fig. 1. Schematic representation of diffraction measurement geometry for two sets of diffracting planes in (a) conventional ( $\theta$ - $2\theta$ ) Bragg-Brentano (BB) geometry and (b) MS beam line synchrotron facility. The incidence of beam with respect to the sample surface ( $\alpha_1$ ) remains same for all diffracting planes at SLS. The stress axis is perpendicular to the plane of figure.

[17,19] have further suggested that atomic shuffles and local diffusion associated with annealing and/or mechanical deformation can reduce local stresses at GBs and triple junctions (TJs), suggesting that the initial high RMS strain of NC metals can be reduced by annealing or deformation.

Although it is difficult to produce NC specimens with controlled grain boundary characteristics, it is possible to produce samples with a strong or a weak texture by electrodeposition. Note that a strong texture is usually associated with a greater fraction of low angle boundaries.

In this study, we investigate the role of RMS strain, GB characteristics and stress orientation on the microplastic deformation in bulk free standing electrodeposited NC Ni by *in situ* mechanical testing with synchrotron x-ray diffraction. Limited transmission electron microscopy was used to obtain the initial grain size distribution. The RMS strain in the samples was varied by isothermal annealing of the NC films at 423 K. The influence of GB characteristics was studied by testing two different NC Ni films with strong and weak texture. Although most experiments were conducted in tension a limited number of experiments were conducted also in compression to examine the role of stress orientation on microplastic flow.

## 2. Experimental methods

Bulk NC Ni samples with two different textures were deposited by a pulse electrodeposition technique:  $Ni_S$  and  $Ni_W$ , with the subscripts S and W corresponding to a strong and weak texture. The details of the electrodeposition conditions are provided in the [Supplementary section ST1](#). Equal amount of saccharin was used as a stress reliever and levelling agent for both materials. The initial  $Ni_S$  and  $Ni_W$  films had a thickness of  $\sim 100 \mu\text{m}$  and 1 mm, respectively.

A combustion analyzer (LECO) with ASTM E 1019-08 standard test method was used to determine the sulphur and carbon content in the deposit. Conventional X-ray diffraction patterns were obtained with a Panalytical Xpert system with Cu-K $\alpha$  radiation. The diffraction profiles for both  $\langle 111 \rangle$  -  $\langle 222 \rangle$  and  $\langle 200 \rangle$  -  $\langle 400 \rangle$  grain families were analyzed using the Warren Averbach method [33] to obtain the scattering domain size and the mean square strain. For the calculation of the latter a scattering column length of 2 nm was used. High resolution SEM measurements reveal the presence of nearly equiaxed grains in both deposits. The strongly textured as-deposited NC samples, listed as  $Ni_S$ -0, were annealed at 423 K for 23 min and 180 min. These samples are listed as  $Ni_S$ -23 and  $Ni_S$ -180, according to the duration of isothermal annealing. The pole figures for  $Ni_S$ -0 and  $Ni_W$  were measured and analyzed with a Bruker Discover-D8 set-up in conjunction with Labotex software. Transmission electron microscopy (TEM) investigations were performed with a Technai F-30, on samples prepared by twin jet polishing at 243 K in a mixture of perchloric acid and ethanol, with a 1:9 volume ratio.

The *in situ* mechanical tests were performed at the Materials Science (MS) beam line of the Swiss Light Source (SLS). Mini dog bone tensile samples with a nominal gage length of 1.7 mm were machined by electro discharge machining (EDM), and subsequently electropolished to remove any damage induced during machining. The samples were subject to load-unload cycles at engineering strain rates of  $5 \times 10^{-4} \text{ s}^{-1}$  and  $1.7 \times 10^{-3} \text{ s}^{-1}$ , respectively, in tension ( $Ni_S$  and  $Ni_W$ ) or compression ( $Ni_W$ ). The compression samples had nominal height of

0.95 mm and square cross-section with sides of  $(0.45 \times 0.48) \text{ mm}^2$ . Details on the mechanical testing frame and beam geometry at SLS are given elsewhere [20]. For all tests a minimum stress of 50 MPa was retained in the unloaded state to ensure proper sample alignment for diffraction measurements. The diffraction patterns were recorded in the loaded and unloaded state during subsequent tensile loading-unloading cycles.

Information on peak position and peak width (full width at half maximum – FWHM), during *in situ* measurements at SLS was obtained by fitting individual peaks with a split Pearson7 function. From the peak positions the elastic lattice strains are obtained as:

$$\varepsilon_{hkl}^{\text{lattice}} = \left( \frac{\Delta d_{hkl}}{d_{hkl}} \right) = -(\cot \theta_{hkl})(\Delta \theta_{hkl}) \quad (1)$$

where  $d_{hkl}$  is the initial lattice plane spacing for  $hkl$  planes,  $\Delta d_{hkl}$  represents the change in lattice plane spacing,  $\theta_{hkl}$  and  $\Delta \theta_{hkl}$  the diffraction peak positions and peak shift, in radians. In order to maintain clarity and track the changes in peak profile, data from four diffraction peaks (111, 200, 220 and 311) were used for the analyses. A classification of grains based on common diffraction vector was used to examine the microstructural changes in various grain families.

It is important to note that two different diffraction geometries were used for the laboratory scale X-ray measurements and for *in situ* studies at the synchrotron, as shown schematically in Fig. 1. For the laboratory based setup the Bragg-Brentano (BB) geometry ( $\theta$ - $2\theta$ ) was used (Fig. 1a). Here the incident beam and detector are rotated in synchronized motion such that the diffracting planes are always parallel to plane of the deposit. For the synchrotron measurements the incident beam and detector configuration are fixed. As a consequence, the orientation of the diffracting planes are different for each grain family (see set 1 and set 2 in Fig. 1b). However, for both configurations diffraction measurements were made on planes with their normal perpendicular to loading direction.

## 3. Experimental results

### 3.1. Microstructure

A wet chemical analysis of the as-deposited NC nickel showed a sulphur and carbon content of 400 ppm and 440 ppm by weight, respectively. Table 1 lists the microstructural parameters calculated from conventional X-ray diffraction measurements in BB-geometry. For all samples the  $\langle 200 \rangle$  reflections showed smaller scattering domain sizes and larger RMS strains than  $\langle 111 \rangle$  reflections. Annealing for short period ( $Ni_S$ -23) caused a rapid reduction in RMS strain with no change in scattering domain size ( $\sim 10 \text{ nm}$ ) for  $\langle 111 \rangle$  grains. Upon further annealing ( $Ni_S$ -180) the mean square strain continued to decrease but also the scattering domain size increased slightly to  $\sim 13 \text{ nm}$ . The behavior of the  $\langle 200 \rangle$  grains was very similar to that of the  $\langle 111 \rangle$  grains, suggesting that recovery is relatively homogeneous during annealing. Note that both the  $Ni_S$ -0 and  $Ni_W$  have a similar grain size and RMS strain.

The bulk texture measurements reveal the presence of the expected fiber texture for both  $Ni_S$  and  $Ni_W$ . Fig. 2 shows inverse pole figures for  $Ni_S$ -0 and  $Ni_W$ , in the growth direction, revealing a strong 200 fiber texture in  $Ni_S$  and a relatively weak texture in  $Ni_W$ . Also, the texture

Download English Version:

<https://daneshyari.com/en/article/5455514>

Download Persian Version:

<https://daneshyari.com/article/5455514>

[Daneshyari.com](https://daneshyari.com)